

Supporting Information

Pentasulfurated Benzene-Cored Asterisks: Relation Between Crystal Structure and Luminescence Properties

Marco Villa,^{a,b} Simone D'Agostino,^a Piera Sabatino,^a Raymond Noel,^b José Busto,^b Myriam Roy,^b Marc Gingras,^b Paola Ceroni^a

^a*Department of Chemistry "Giacomo Ciamician", Via Selmi, 2, 40126 Bologna, Italy*

^b*Aix Marseille Univ, CNRS, CINaM, Marseille, France*

Materials and General Procedures

All reagents, solvents and chemicals were purchased from Sigma-Aldrich, Fisher or Alfa-Aesar and used directly unless otherwise stated (purity: reagent or analytical grade). Solvents were stored for several days over freshly activated 3 Å molecular sieves (activated for 3 h at 250 °C). All the reactions were monitored by thin-layer chromatography, LC, LCMS or FT-IR (ATR).

Photophysical Measurements

The experiments were carried out in air-equilibrated solution at 298 K unless otherwise noted. Luminescence measurements at 77 K were performed in dichloromethane/methanol (1:1 v/v). UV-vis absorption spectra were recorded with a PerkinElmer I40 spectrophotometer using quartz cells with path length of 1.0 cm. Luminescence spectra were performed with a PerkinElmer LS-50 or an Edinburgh FLS920 spectrofluorimeter equipped with a Hamamatsu R928 phototube. Lifetimes shorter than 10 μs were measured by the above-mentioned Edinburgh FLS920 spectrofluorimeter equipped with a TCC900 card for data acquisition in time-correlated single-photon counting experiments (0.5 ns time resolution) with a 340 nm pulsed diode and a LDH-P-C405 pulsed diode laser. Longer lifetimes were measured by the PerkinElmer LS-50. Emission quantum yields were measured following the method of Demas and Crosby¹ (standard used: [Ru(bpy)₃]²⁺ in aqueous solution)². For solid samples, emission quantum yield was calculated from corrected emission spectra registered by an Edinburgh FLS920 spectrofluorimeter equipped with a barium sulfate coated integrating sphere (4 in.), a 450W Xe lamp (λ excitation tunable by a monochromator supplied with the instrument) as light source, and a R928 photomultiplier tube, following the procedure described by De Mello et al.³

Photophysical characterization in the absence of oxygen was carried out on samples of dye solutions after degassing them by freeze-pump-thaw cycling ($P = 10^{-9}$ Bar; liquid nitrogen as cooling medium) in a custom-made quartz cuvette.

The estimated experimental errors are 2 nm on the band maximum, 5% on the molar absorption coefficient and luminescence lifetime, 10% on the emission quantum yield in solution, and 20% on the emission quantum yield in solid.

Thin-Layer chromatography (TLC): TLC analyses were performed on precoated silica gel (Alugram® SilG/UV254gel) aluminium plates from Macherey-Nagel. Compounds were visualized with UV-light (254 or 365 nm)

Flash chromatography was performed over silica gel 60, Merck type 230-400 mesh (40-63µm).

NMR spectra ¹H (399.78 MHz) and ¹³C (100.53 MHz) were recorded on JEOL ECX-400 spectrometer. Signals of the residual protic solvent CHCl₃ at 7.26 ppm and DMSO-*d*₆ at 2.50 ppm were used as internal references, along with TMS. As for ¹³C NMR spectra, the central resonance of the triplet for CDCl₃ at 77.16 ppm and the signal for DMSO-*d*₆ at 39.52 ppm were used as internal references.⁴ The resonance multiplicities in the ¹H NMR spectra are described as “s” (singlet), “d”(doublet), “t” (triplet), “q” (quarted), “sept” (septet) “m” (multiplet) or “b” (broad).

LC-MS (APCI and ESI): Analyses were performed with a C18 Phenomenex Luna (3 µm; 100 x 2 mm) column on a Shimadzu LCMS-2020 fitted with two LC-20AD prominence pumps equipped with a DGU-20AD prominence line degasser, a SIL-20AHT prominence auto-sampler, a CTO-20A prominence column oven, a SPD-20A prominence UV/Vis detector, a FCV-20AH valve unit, a Parker NitroFloLab nitrogen generator and either an APCI SET or an ESI SET detector. Positive or negative modes were used for both APCI and ESI mode.

HRMS (ESI): High resolution mass spectra were recorded at the Spectropôle de Marseille (France) in triplicate with double internal standards. Oligomers of poly(propylene glycol) were used as internal standards. Ionization was facilitated by some adducts with Ag⁺, NH₄⁺ or Na⁺ ions. Two spectrometers were used: a) SYNAPT G2 HDMS (Waters) instrument equipped with an ESI source and a TOF analyzer in a positive mode. b) QStar Elite (Applied Biosystems SCIEX) instrument equipped with an atmospheric ionization source (API). The samples were ionized under ESI with an electrospray voltage of 5500 V; orifice voltage: 10 V, and air pressure of the nebulizer at 20 psi. A TOF analyzer was used in a positive mode.

FT-IR: Infrared absorption spectra were directly recorded on solids or neat liquids on a Perkin-Elmer Spectrum 100 FT-IR Spectrometer equipped with a universal ATR accessory (contact crystal: diamond).

Elemental analysis: Elemental analyses were performed by the Spectropôle of Marseille on a Thermo Finnigan EA 1112 equipped with an autosampler and Eager Xperience software.

Experimental

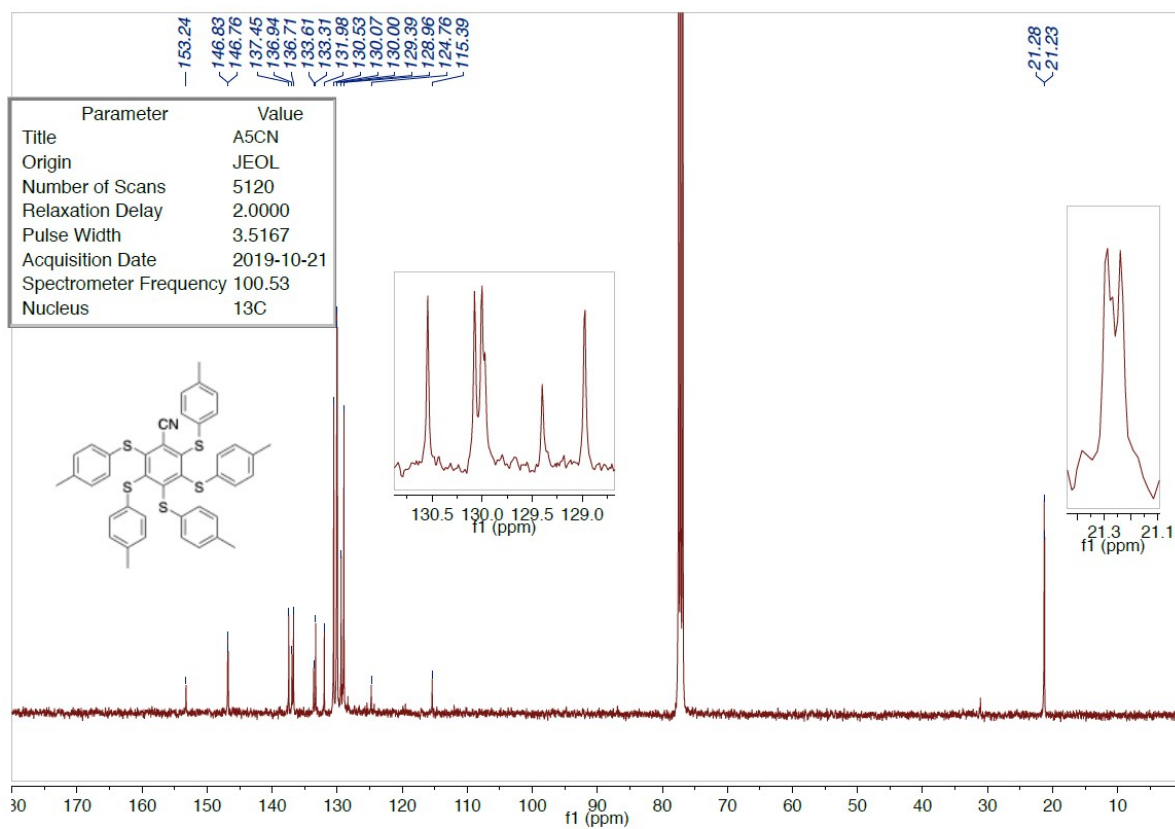
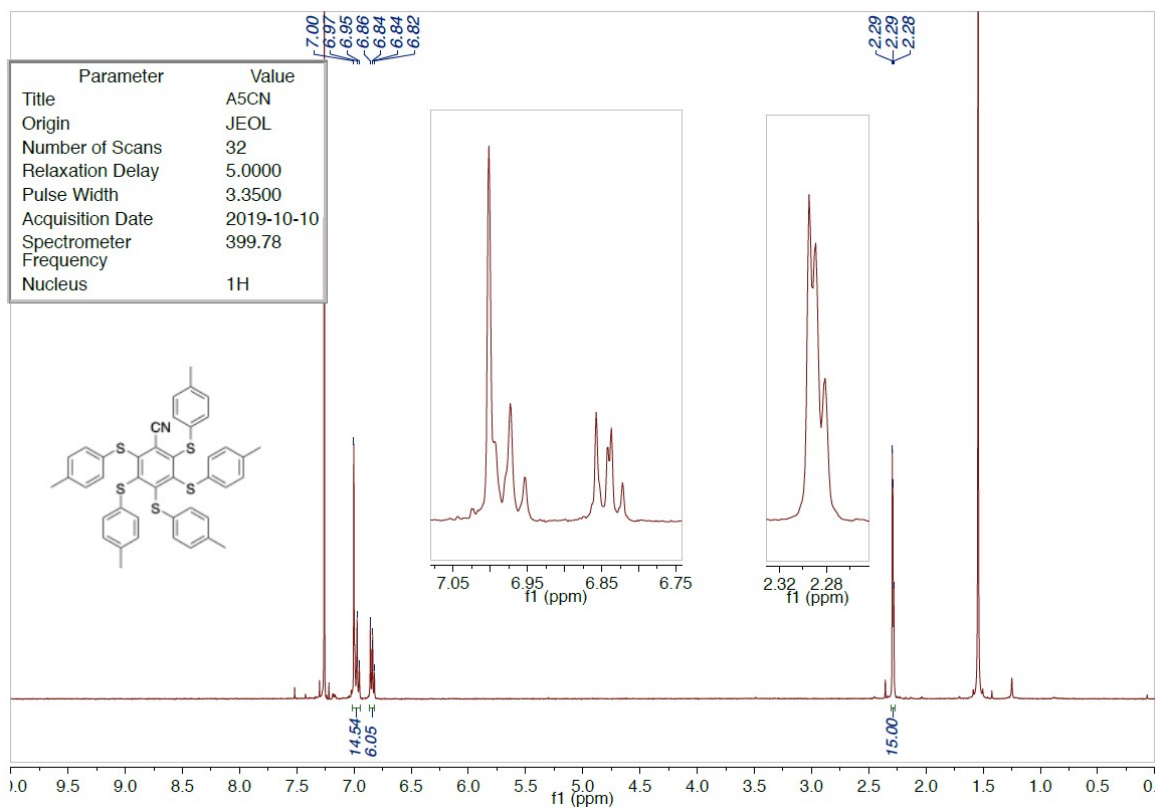
2,3,4,5,6-pentakis(p-tolylthio)benzonitrile (A5CN): to a solution of 2,3,4,5,6-pentafluorobenzonitrile (106 mg, 0.549 mmol, 1.0 eq.) in dry DMF (4 mL) was added K₂CO₃ (572 mg 4.139 mmol, 7.5 eq.). The mixture was purged with Argon. The 4-methylbenzenethiol (482 mg, 3.881 mmol, 7.1 eq.) was then added and the reaction mixture was stirred at room temperature overnight. The reaction mixture turned bright yellow. Upon completion of the reaction, the reaction mixture was diluted with 50 mL of 2M NaOH (aq.) and extracted 3 times with DCM (3 x30 mL). The organics layers were combined, dried over MgSO₄, filtered and concentrated *in vacuo*. The crude product was purified by column chromatography over silica gel using petroleum ether (PE)/DCM as eluent. The desired product **A5CN** was obtained as a bright-yellow solid (370 mg, 518 µmol, 94 %). **TLC** (SiO₂, PE:DCM; 8:2 v/v) R_f:0.16; **¹H NMR** (399.78 MHz, CDCl₃, ppm) δ= 7.01-6.94 (m, 14H), 6.84 (d,

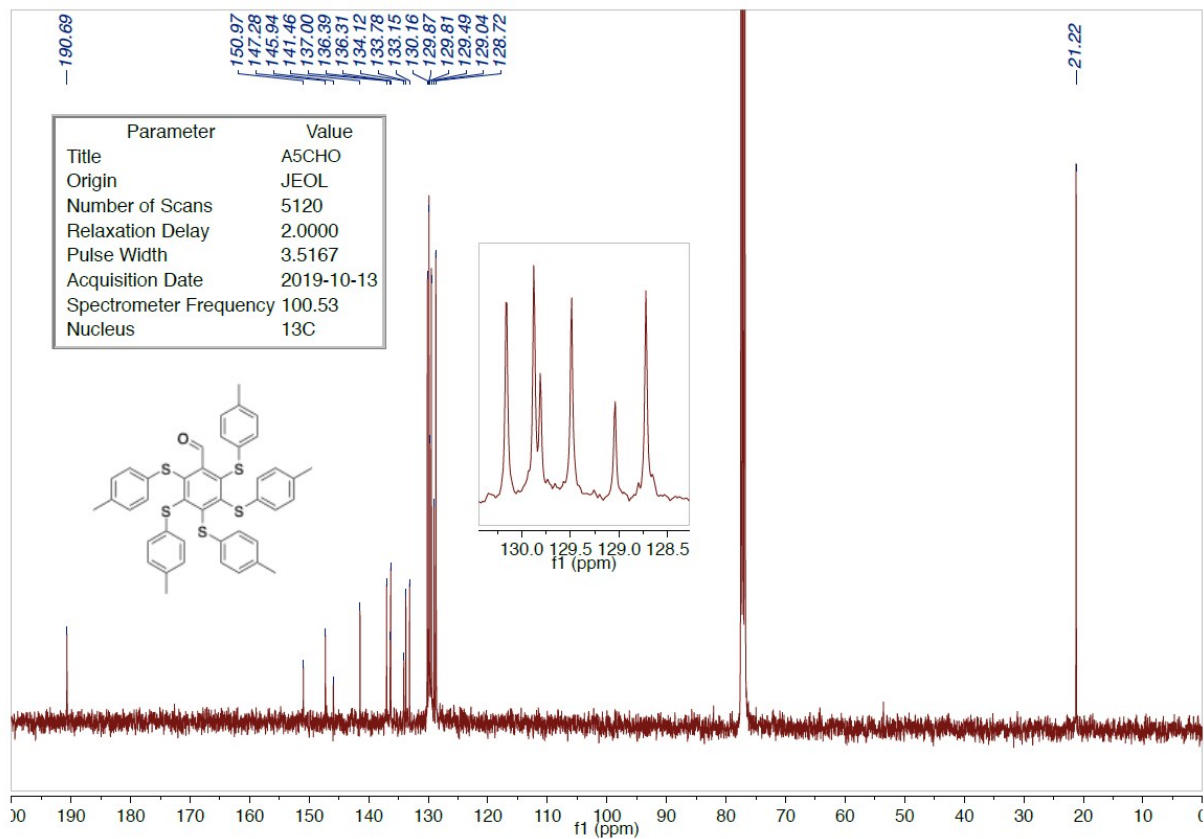
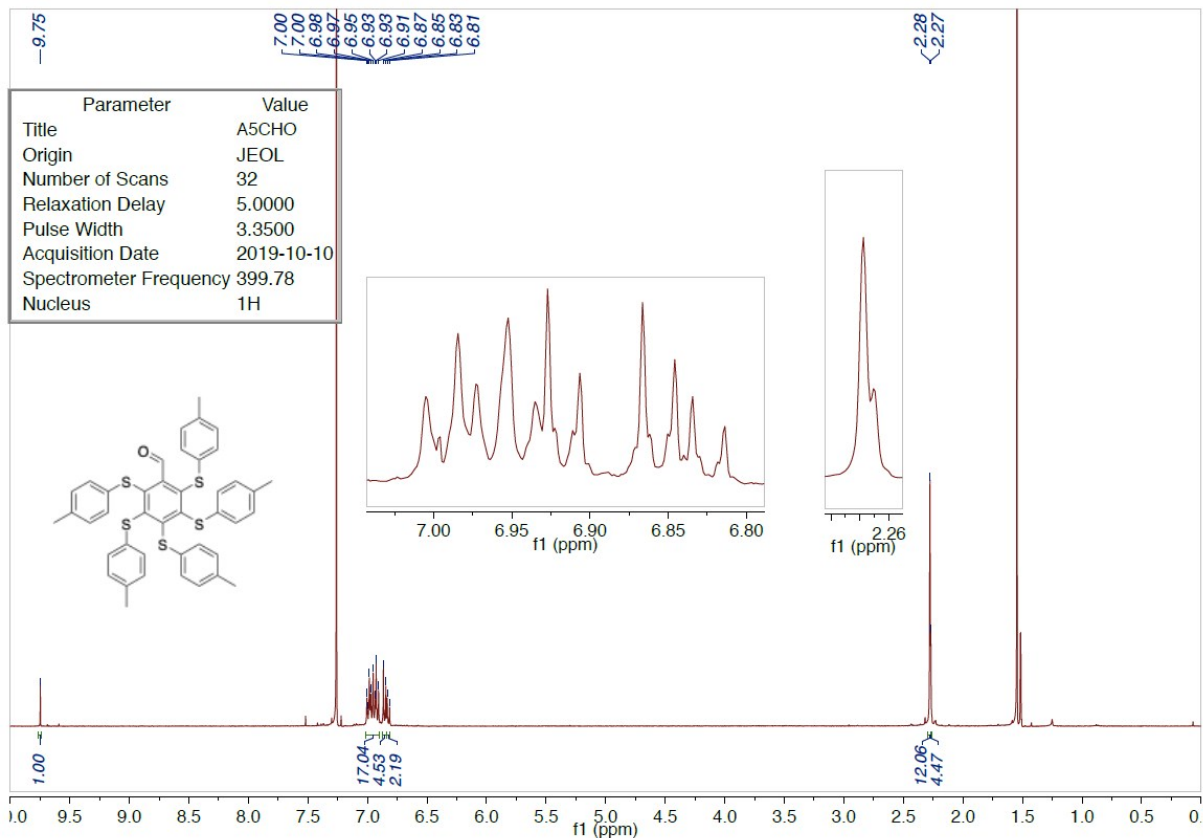
$J = 8.2$ Hz, 4H), 6.82 (d, $J = 8.0$ Hz, 2H), 2.295 (s, 6H), 2.290 (s, 6H), 2.28 (s, 3H); ^{13}C NMR (100.53 MHz, CDCl_3 , ppm) $\delta = 153.24, 146.83, 146.76, 137.45, 136.94, 136.71, 133.61, 133.31, 131.98, 130.53, 130.07, 130.00, 129.97, 129.39, 128.96, 124.76, 115.39, 21.28, 21.27, 21.23$; HRMS (API+) calculated for $[\text{C}_{42}\text{H}_{35}\text{NS}_5 + \text{NH}_4^+]$: 731.11 Da, found $[\text{M} + \text{NH}_4^+]$ 731.1712 m/z .

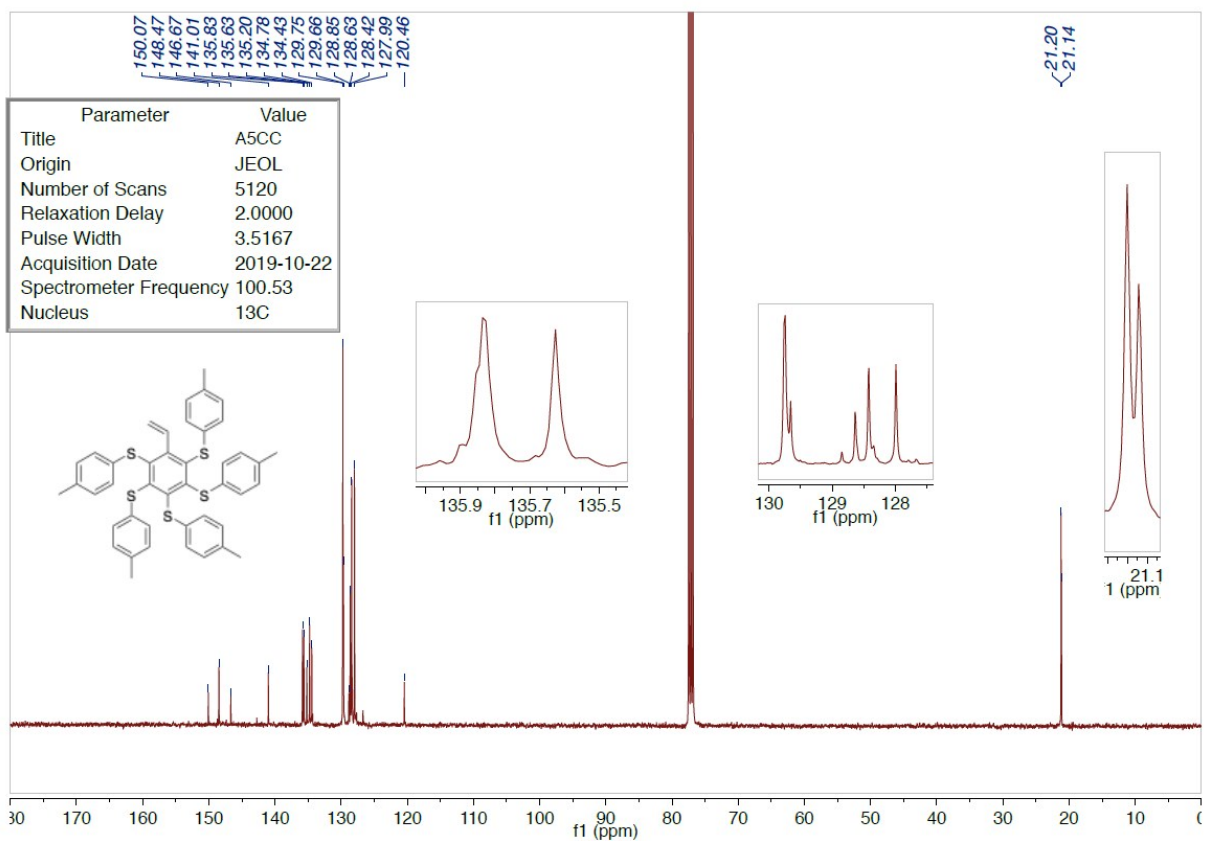
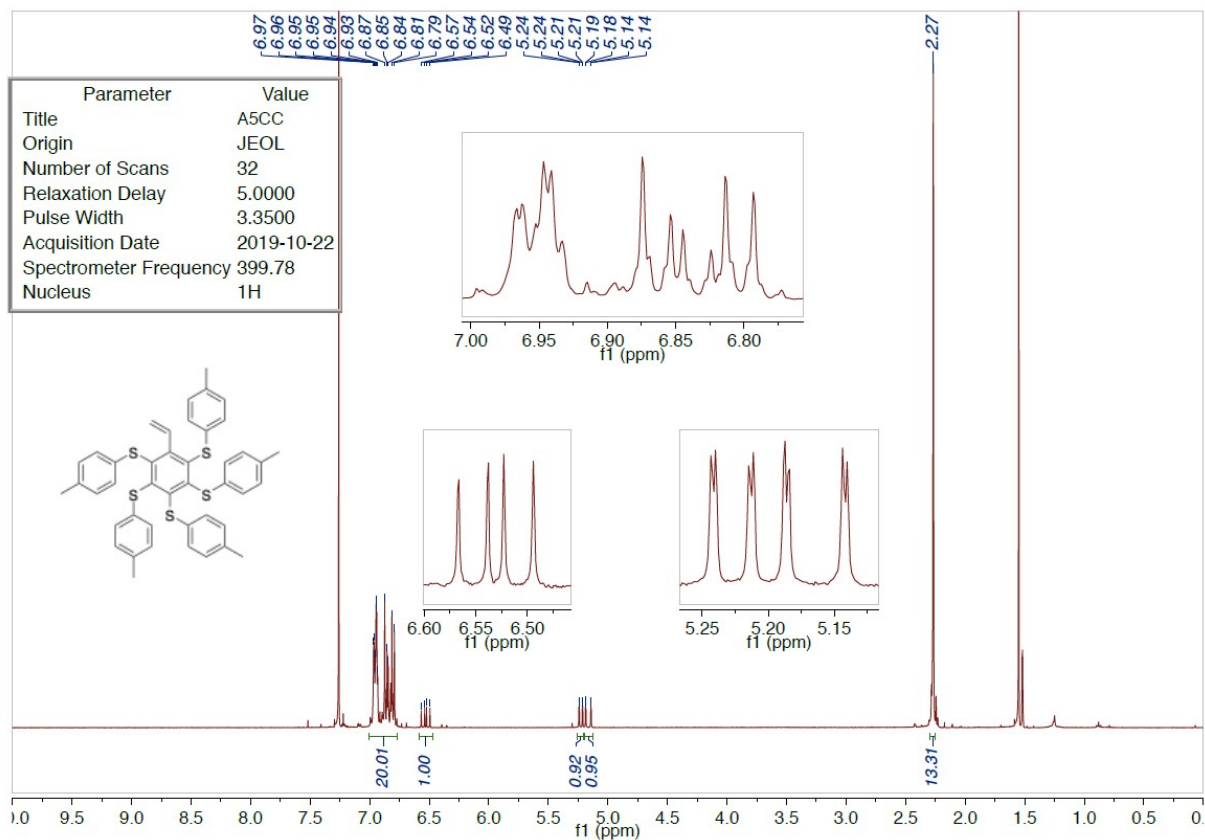
2,3,4,5,6-pentakis(p-tolylthio)benzaldehyde (A5CHO): Pentafluorobenzaldehyde (500 mg, 2.55 mmol, 1.0 eq.) was dissolved in dry DMI (6 mL), K_2CO_3 (2.82 g 20.4 mmol, 8.0 eq.) was added. The mixture was purged with Argon. The mixture turned yellow. The 4-methylbenzenethiol (2.37 g, 19.1 mmol, 7.5 eq.) was added, and the reaction turned orange. The reaction mixture was heated to 40 °C and stirred overnight. Upon completion of the reaction, the mixture was treated with NaOH 2 M (100 mL) and extracted with Et_2O (5 x 20 mL). The organics layers were combined, dried over MgSO_4 and filtered. After removal of the solvent, the brown orange oil was purified by column chromatography over silica gel using cyclohexane/dichloromethane as eluent. Compound **A5CHO** was obtained as an orange-yellow solid (1.65 g, 90 %). ^1H NMR (399.78 MHz, CDCl_3 , ppm) $\delta = 9.75$ (s, 1H), 6.99 (d, $J = 8.3$ Hz, 4H), 6.96 (d, $J = 8.2$ Hz, 4H), 6.94 (d, $J = 8.3$ Hz, 2H), 6.92 (d, $J = 8.3$ Hz, 4H), 6.86 (d, $J = 8.3$ Hz, 4H), 6.82 (d, $J = 8.3$ Hz, 2H), 2.28 (s, 12H), 2.27 (s, 3H); ^{13}C NMR (100.53 MHz, CDCl_3 , ppm) $\delta = 190.69, 150.97, 147.28, 145.94, 141.46, 137.00, 136.39, 136.31, 134.12, 133.78, 133.15, 130.16, 129.87, 129.81, 129.49, 129.04, 128.72, 21.22$ (3C); HRMS (ESI-MS): 716.1370 Da +/- 1 ppm IR (ν , cm^{-1} , neat): 3018 (w), 2917 (w), 2862 (w), 1889 (w) 1698 (m), 1566 (w), 1489 (s), 1447(m), 1286 (m), 1162 (m), 1083 (m), 1015 (m), 926 (m), 796 (s), 734(m), 700 cm^{-1} (m).

(6-vinylbenzene-1,2,3,4,5-pentayl)pentakis(p-tolylsulfane) (A5CC): The Methyltriphenylphosphonium bromide salt (598 mg, 1.67 mmol, 1.2 eq.) was suspended in dry THF and was cooled to 0 °C. The n-buthyllithium (1.53 mmol, 1.1 eq.) was added at 0 °C. After the addition of the butyllithium the mixture was warmed up to room temperature for 5 minutes, the reaction turned dark red and was cooled back to 0 °C. Then, **A5CHO** (1 g, 1.39 mmol, 1.0 eq.) was added to the reaction at 0 °C. The reaction turned black. After 2 h the solvent was evaporated, and the residue was taken in Et_2O in order to precipitate the phosphine oxide and filtered. Ether was evaporated, the residue was purified over silica gel. Compound **A5CC** was obtained as an intense yellow solid (84 %). ^1H NMR (100.53 MHz, CDCl_3 , ppm) $\delta = 7.00 - 6.76$ (m, 20H), 6.49 (dd, $J = 17.6, 11.5$ Hz, 1H), 5.21 (dd, $J = 11.5, 1.4$ Hz, 1H), 5.14 (dd, $J = 17.5, 1.4$ Hz, 1H), 2.28 (s, 15H CH_3). ^{13}C NMR (100.53 MHz, CDCl_3 , ppm) $\delta = 150.07, 148.47, 146.67, 141.01, 135.84, 135.83, 135.63, 135.20, 134.78, 134.43, 129.75$ (2C), 129.66, 128.85, 128.63, 128.42, 127.99, 120.46, 21.20 (2C), 21.14. HRMS: 714.1577 Da +/- 1 ppm IR (ν , cm^{-1} , neat): 3017 (w), 2917 (w), 2862 (w), 1887 (w), 1566 (w), 1489 (s), 1447(m), 1280 (w), 1179 (m), 1084 (m), 1016 (m), 921 (w), 796 (s), 736(m), 698 cm^{-1} (m); EA($\text{C}_{43}\text{H}_{38}\text{S}_5$) : calculated : 72.23 %C 5.36 %H 0 %O 22.42 %S, found: 72.30 %C 5.37 %H 0 %O 22.08 %S.

¹H and ¹³C NMR spectra of A5CN, A5CHO and A5CC







X-ray Diffraction

Single-crystal data for all compounds were collected at RT, except **A5CN** (see next section) and **A5CHO** for which an additional dataset was collected at 100 K, on an Oxford XCalibur S CCD diffractometer equipped with a graphite monochromator (Mo-K α radiation, $\lambda = 0.71073\text{\AA}$). The structures were solved by intrinsic phasing with SHELXT⁵ and refined on F^2 by full-matrix least squares refinement with SHELXL implemented in Olex2 software.⁶ All non-hydrogen atoms were refined anisotropically applying the rigid-body RIGU restraint.⁷ H_{CH} atoms for all compounds were added in calculated positions and refined riding on their respective carbon atoms. Data collection and refinement details are listed in Table S1. The program Mercury⁸ was used to calculate intermolecular interactions and for molecular graphics. Crystal data can be obtained free of charge via www.ccdc.cam.ac.uk/conts/retrieving.html (or from the Cambridge Crystallographic Data Centre, 12 Union Road, Cambridge CB21EZ, UK; fax: (+44)1223-336-033; or e-mail: deposit@ccdc.cam.ac.uk). CCDC numbers 1958552-1958555.

For phase identification purposes X-ray powder diffractograms in the 2θ range 5–40° (step size, 0.02°; time/step, 20 s; 0.04 rad soller; 40mA x 40kV) were collected on a Panalytical X'Pert PRO automated diffractometer equipped with an X'Celerator detector and in Bragg-Brentano geometry, using Cu K α radiation without a monochromator. The program Mercury⁸ was used for simulation of X-ray powder patterns on the basis of single crystal data. In all cases, the identity between polycrystalline samples and single crystals was always verified by comparing experimental and simulated powder diffraction patterns (See Figure S1).

XRPD analysis of A5CN was performed on a PANalytical X'Pert Pro automated diffractometer equipped with a PIXcel detector in transmission geometry (capillary spinner), using Cu-K α radiation ($\lambda = 1.5418\text{\AA}$) without monochromator in the 2θ range between 3° and 70°s (continuous scan mode, step size 0.0260°, counting time 889.70 s, Soller slit 0.02, antiscatter slit $\frac{1}{4}$, divergence slit $\frac{1}{4}$, 40 mA*40kV). 6 patterns were recorded and summed to enhance the signal to noise ratio. Powder diffraction data were analyzed with the software EXPO2014,⁹ which is designed to analyze both monochromatic and non-monochromatic data. Selected peaks were chosen in the 2θ range 5–50°, and a monoclinic cell with a volume of ca. 1800 \AA^3 (see Table S1) was found using the algorithm N-TREOR09.¹⁰ The structure was solved by simulated annealing employing a fragment derived from the structure of A5CHO, previously solved through single-crystal XRD, and refined as a rigid body with the software EXPO2014.⁹ A shifted Chebyshev function with 12 parameters and a Pseudo-Voigt function were used to fit background and peak shape, respectively. An overall thermal parameter for all the atoms was adopted. Refinement converged with GOF = 3.9, Rwp = 7.2%, Rp = 5.1%. See Figure S2.

Table S1. Crystal data and refinement details for crystalline **A5CN**, **A5CHO** (both at RT and LT), and **A5CC**.

| | A5CN | A5CHO (RT) | A5CHO (100K) | A5CC |
|---|--|--|--|--|
| Formula | C ₄₂ H ₃₅ S ₅ N | C ₄₂ H ₃₆ S ₅ O | C ₄₂ H ₃₆ S ₅ O | C ₄₃ H ₃₈ S ₅ |
| fw | 714.076 | 717.01 | 717.01 | 715.03 |
| Temperature (K) | RT | RT | 100 | RT |
| Cryst. System | Monoclinic | Monoclinic | Monoclinic | Monoclinic |
| Space group | P2 ₁ | P2 ₁ | P2 ₁ | P2 ₁ |
| Z | 2 | 2 | 2 | 2 |
| a (Å) | 12.931(4) | 13.174(2) | 12.9947(19) | 13.507(3) |
| b (Å) | 5.892(1) | 5.893(1) | 5.790(1) | 5.924(1) |
| c (Å) | 23.919(7) | 23.803(2) | 23.584(3) | 23.648(5) |
| α (deg) | 90 | 90 | 90 | 90 |
| β (deg) | 94.155(1) | 94.46(1) | 94.710(12) | 94.45(2) |
| γ (deg) | 90 | 90 | 90 | 90 |
| V (Å ³) | 1817.4(1) | 1842.6(5) | 1768.4(5) | 1886.5(7) |
| D _{calc} (g/cm ³) | 1.305 | 1.292 | 1.347 | 1.259 |
| μ (mm ⁻¹) | 0.316 | 0.347 | 0.362 | 0.337 |
| Measd reflns | 934 | 7181 | 6986 | 6942 |
| Indep reflns | - | 4244 | 4476 | 5287 |
| Largest diff. peak/hole (e/Å ³) | - | 0.21/-0.22 | 0.30/-0.31 | 0.20/-0.19 |
| R ₁ [on F _o ² , I>2σ(I)] | - | 0.0786 | 0.0884 | 0.0721 |
| wR ₂ (all data) | - | 0.1622 | 0.1590 | 0.1612 |
| R _p (%) | 5.1 | - | - | - |
| R _{wp} (%) | 7.2 | - | - | - |

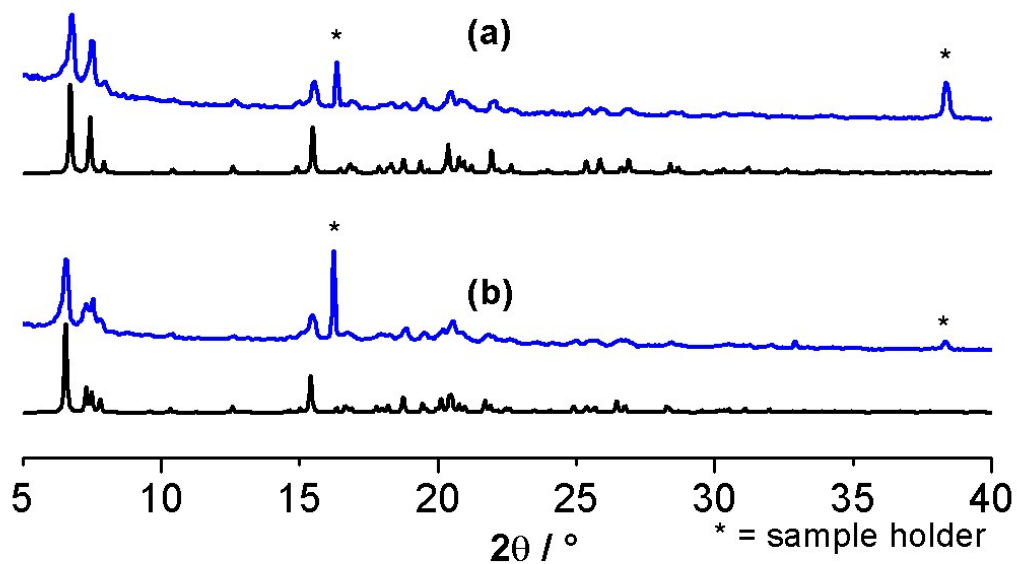


Figure S1. Comparison of the experimental XRPD patterns (blue-line) with those calculated (black-line) on the basis of single crystal data for compounds: (a) **A5CHO**, and (b) **A5CC**.

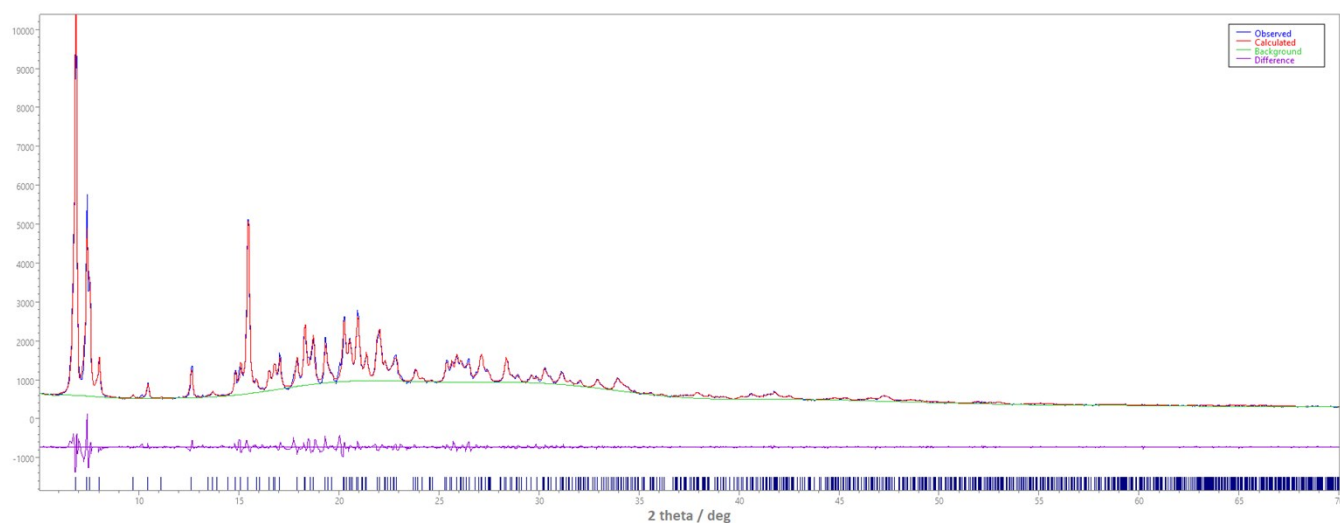


Figure S2. Experimental (blue), calculated (red) XRPD pattern of **A5CN** by Rietveld refinement and difference profile (magenta).

References

1. G. A. Crosby and J. N. Demas, *J. Phys. Chem.*, 1971, **75**, 991-1024.
2. K. Suzuki, A. Kobayashi, S. Kaneko, K. Takehira, T. Yoshihara, H. Ishida, Y. Shiina, S. Oishi and S. Tobita, *PCCP*, 2009, **11**, 9850-9860.
3. J. C. de Mello, H. F. Wittmann and R. H. Friend, *Adv. Mater.*, 1997, **9**, 230-232.
4. G. R. Fulmer, A. J. M. Miller, N. H. Sherden, H. E. Gottlieb, A. Nudelman, B. M. Stoltz, J. E. Bercaw and K. I. Goldberg, *Organometallics*, 2010, **29**, 2176-2179.
5. G. M. Sheldrick, *ActaCryst.*, 2015, **A71**, 3-8
6. O. V. Dolomanov, L. J. Bourhis, R. J. Gildea, J. A. K. Howard, H. Puschmann, *J. Appl. Crystallogr.* 2009, **42**, 339-341.
7. A. Thorn, B. Dittrich, G. M. Sheldrick, *Acta Cryst.*, 2012, **A68**, 448-451.
8. C. F. Macrae, I. J. Bruno, J. A. Chisholm, P. R. Edgington, P. McCabe, E. Pidcock, L. Rodriguez-Monge, R. Taylor, J. v. d. Streek and P. A. Wood, *J. Appl. Crystallogr.*, 2008, **41**, 466-470.
9. A. Altomare, C. Cuocci, C. Giacovazzo, A. Moliterni, R. Rizzi, N. Corriero and A. Falcicchio, *J. Appl. Crystallogr.*, 2013, **46**, 1231-1235.
10. A. Altomare, C. Giacovazzo, A. Guagliardi, A. G. Moliterni, R. Rizzi and P.-E. Werner, *J. Appl. Crystallogr.*, 2000, **33**, 1180-1186.